THE JOURNAL OF BIOLOGICAL CHEMISTRY VOL. 281, NO. 50, pp. 38689–38696, December 15, 2006

Single Molecule Force Spectroscopy of Salt-dependent Bacteriophage T7 Gene 2.5 Protein Binding to Single-stranded DNA*

Received for publication, September 5, 2006, and in revised form, October 16, 2006 Published, JBC Papers in Press, October 17, 2006, DOI 10.1074/jbc.M608460200

Leila Shokri[‡], Boriana Marintcheva[§1], Charles C. Richardson[§], Ioulia Rouzina[¶], and Mark C. Williams[‡‖2]

From the [‡]Department of Physics and [‖]Center for Interdisciplinary Research on Complex Systems, Northeastern University, Boston, Massachusetts 02115, the [§]Department of Biological Chemistry and Molecular Pharmacology, Harvard Medical School, Boston, Massachusetts 02115, and the [¶]Department of Biochemistry Molecular Biology and Biophysics, University of Minnesota, Minneapolis, Minnesota 55455

The gene 2.5 protein (gp2.5) encoded by bacteriophage T7 binds preferentially to single-stranded DNA. This property is essential for its role in DNA replication and recombination in the phage-infected cell. gp2.5 lowers the phage λ DNA melting force as measured by single molecule force spectroscopy. T7 gp2.5-Δ26C, lacking 26 acidic C-terminal residues, also reduces the melting force but at considerably lower concentrations. The equilibrium binding constants of these proteins to single-stranded DNA (ssDNA) as a function of salt concentration have been determined, and we found for example that gp2.5 binds with an affinity of $(3.5 \pm 0.6) \times 10^5$ M^{-1} in a 50 mM Na^+ solution, whereas the truncated protein binds to ssDNA with a much higher affinity of $(7.8 \pm 0.9) \times 10^7$ M^{-1} under the same solution conditions. T7 gp2.5-Δ26C binding to single-stranded DNA also exhibits a stronger salt dependence than the full-length protein. The data are consistent with a model in which a dimeric gp2.5 must dissociate prior to binding to ssDNA, a dissociation that consists of a weak non-electrostatic and a strong electrostatic component.

Optical tweezers have been used extensively for studying the biomechanical properties of single DNA molecules by stretching the molecules and measuring the required force for a given extension under various conditions (1–6). The mechanical work performed by stretching has an energy scale of the noncovalent interactions that hold the two DNA strands together (7) and can therefore be used to induce conversion of double-stranded DNA (dsDNA)[3] into single-stranded DNA (ssDNA). When this mechanical process is reversible, the calculated work is equal to the equilibrium melting free energy (7–9).

The method of ssDNA stretching in which two strands are melted by force is referred to as force-induced melting (FIM). This method provides valuable information regarding the interaction between nucleic acids and proteins or small molecules that bind to DNA (9). In the experiments described here, a single λ-DNA molecule of 48,500 base pairs was stretched to extensions that were almost twice its B-form contour length, resulting in a FIM transition. Extended regions of dsDNA melt cooperatively, and the midpoint of the melting transition, F_m, is analogous to the DNA melting temperature, T_m, obtained in thermal melting studies. F_m, like T_m, is similarly affected by solution conditions such as pH, temperature, and ionic strength (5, 9, 10). DNA-binding proteins and small molecules that affect the thermal melting equilibrium of dsDNA affect the FIM transition in a similar manner (9, 11–17). One advantage of the FIM method is that DNA melting studies can be performed over a wide range of temperatures, including physiological temperature, thus avoiding protein denaturation. In addition, because the DNA is stretched during the single molecule experiment, measurements can be obtained under solution conditions that would allow the protein-DNA complex to aggregate in a bulk solution experiment.

In previous work, we used DNA stretching to probe the interactions of T4 gene 32 protein (gp32) to ssDNA. We used this method to determine the association constant of gp32 to ssDNA over a range of salt concentrations, including physiological conditions (11–13). Surprisingly, we found that the association constant of wild type gp32 exhibited very little salt dependence below 200 mM Na^+, in contrast to bulk experiments, which had previously shown a very strong salt dependence in high salt. A C-terminal truncation of gp32, denoted *I, does not show salt-independent binding at low salt. We proposed that the lack of salt dependence to wild type gp32-ssDNA binding in low salt was due to a conformational change involving the acidic C-terminal domain of gp32, which may be required for gp32-ssDNA binding (18, 19). Because this conformational change begins to strongly alter gp32 binding near physiological salt concentrations, we had previously proposed that the C-terminal domain of gp32 may act as a regulatory switch. The presence of an acidic C terminus is a common feature of all prokaryotic and mitochondrial ssDNA-binding

* This work was supported in part by National Institutes of Health Grants GM 72462 (to M. C. W.) and GM 54397 (to C. C. R.), National Science Foundation Grant MCB-0238190 (to M. C. W.), and United States Department of Energy Grant DE-FG02-96ER62251 to (to C. C. R.). The costs of publication of this article were defrayed in part by the payment of page charges. This article must therefore be hereby marked "*advertisement*" in accordance with 18 U.S.C. Section 1734 solely to indicate this fact.

[1] Supported by National Institutes of Health Postdoctoral Fellowships ST32A107245-20 and F32GM72305T.

[2] To whom correspondence should be addressed: Dept. of Physics and Center for Interdisciplinary Research on Complex Systems, Northeastern University, 111 Dana Research Ctr., Boston, MA 02115. Tel.: 617-373-7323; Fax: 617-373-2943; E-mail: mark@neu.edu.

[3] The abbreviations used are: dsDNA, double-stranded DNA; ssDNA, single-stranded DNA; gp2.5, T7 gene 2.5 protein; CTT, C-terminal tail; FIM, force-induced melting.

proteins, which have been shown to modulate the DNA binding properties of the proteins and mediate protein-protein interactions (20). However, the replication systems that contain these proteins may differ substantially. For example, the T7 replication system is very economical and can be reconstituted *in vitro* with only four proteins: DNA polymerase with its processivity factor, thioredoxin, the helicase/primase, and the ssDNA-binding protein, which are involved in multiple protein-protein interactions within the phage replisome. In contrast, T4 phage replication employs a different set of replication proteins, as well as several additional accessory proteins. The differences in complexity between these two systems suggest the possibility of more sophisticated coordination between the DNA binding properties of the single-stranded binding protein from T7, gp2.5, and the protein-protein interactions with other T7 replication proteins. Therefore, we now present a single molecule study of salt-dependent ssDNA binding by the single-stranded DNA-binding protein from bacteriophage T7 in order to examine the differences between the DNA binding activities of T4 gp32 and T7 gp2.5.

Bacteriophage T7 gene 2.5 protein (gp2.5), encoded by gene 2.5 of the bacteriophage T7, is a ssDNA-binding protein (21). It physically interacts with both T7 DNA polymerase and the T7 helicase/primase (22–26) and plays multiple roles in T7 DNA replication and recombination (22, 27–36). In the absence of DNA, gp2.5 forms a stable homodimer in solution (35). Its nucleic acid and protein interactive properties are strongly dependent on the domain structure of the protein (22, 24–26, 29, 37, 38). The crystal structure of gp2.5 reveals a core that consists of a conserved OB-fold (oligosaccharide/oligonucleotide-binding fold) that is well adapted for interactions with ssDNA. gp2.5 has a highly acidic C-terminal tail that is required for dimer formation and for interactions with T7 DNA polymerase and the helicase/primase (39). A genetically altered protein, gp2.5-Δ26C, lacks the C-terminal 26 residues. gp2.5-Δ26C binds ssDNA more tightly than does the full-length protein (22). Models have been proposed in which the C-terminal tail of gp2.5 interacts with the DNA-binding core of the protein (39, 40).

We utilize DNA stretching to investigate the effects of full-length gp2.5 as well as gp2.5-Δ26C on DNA duplex stability and melting. In accord with the known preferential binding to ssDNA, both proteins reduce the melting force. However, the differences between force-extension curves during stretching and relaxation, (*i.e.* stretching hysteresis), in the presence of both proteins indicates that the system does not reach equilibrium on the time scale of our experiment. The technical limitations of our instrument made it difficult to pull slowly enough to reproduce the complete equilibrium DNA stretching curve. Therefore, we measured the equilibrium force at the midpoint of the DNA melting transition, at the extension corresponding to the melting of half of the base pairs. To do this, we rapidly stretched the dsDNA to a fixed end-to-end extension halfway between the dsDNA and ssDNA contour lengths and monitored the force, which converged to equilibrium at this given extension, on the time scale of several minutes. We then calculated the equilibrium binding constants of the protein to ssDNA from the protein concentration dependence of the measured equilibrium DNA melting force (7, 8, 13).

We found that the binding affinity of the full-length gp2.5 and its C-terminal truncation for exposed ssDNA regions were salt-dependent and differed by several orders of magnitude in low salt. To explain this difference in binding affinity, we developed a model in which a salt-dependent dimerization interaction must be broken in order for gp2.5 to bind to DNA. We then quantified this binding interaction as a function of salt concentration; herein we discuss its relevance to gp2.5 interactions with other T7 replication proteins.

EXPERIMENTAL PROCEDURES

Protein Preparation and Purification—Wild type gp2.5 and gp2.5-Δ26C were purified from BL21(DE3)pLysS cells overexpressing a histidine-tagged version of their genes as described previously (40). Following the purification the histidine tag was proteolytically cleaved using PreScission protease (glutathione *S*-transferase-tagged, Amersham Biosciences). The cleaved histidine tag and the protease were subsequently removed using nickel-nitrilotriacetic acid-agarose (Qiagen) and GSTTrap™ HP columns, respectively. The purified proteins were dialyzed against storage buffer (50 mM Tris-HCL, pH 7.5, 0.1 EDTA, 1 mM dithiothreitol, 50% glycerol) and stored at −20 °C. The storage buffer for gp2.5-Δ26C contained additional 150 mM NaCl. For experiments requiring high concentrations of gp2.5, the protein solution was concentrated using an Amicon Ultra centrifugal filter device (Millipore) with 10-kDa cut-off.

DNA Stretching—The dual-beam optical tweezers instrument used in this study consists of two counter-propagating diode lasers, each with 200 milliwatts of 830 nm light (JDS Uniphase, San Jose, CA) that are convergently directed and focused to a small spot inside a liquid flow cell, using ×60, 1.0 numerical aperture water immersion microscope objectives (Nikon, Tokyo) that form the optical trap. The light leaving the trap is directed onto a lateral effect photodiode detector (UDT Sensors, Hawthorne, CA), which determines the deflection of each beam and outputs a voltage that is directly proportional to the force being exerted on the bead in the optical trap.

To tether single DNA molecules, two 5-μm streptavidin-coated polystyrene beads (Bangs Laboratories, Fishers, IN) were trapped in the optical tweezers and on the end of a glass micropipette (World Precision Instrument, Sarasota, FL). A very dilute solution containing bacteriophage λ-DNA (~ 48,500 base pairs, biotin-labeled on each 3′ terminus), typically in 10 mM Hepes, pH 7.5, and varying NaCl concentrations, was run through the cell until one molecule was captured between the two beads. The flow cell, and thus the glass micropipette, may be moved using a feedback-compensated piezoelectric stage (Melles Griot), causing the single DNA molecule to stretch between two beads, resulting in a force measurement, as described previously (10). The position measurements were converted to a measurement of the molecular extension by correcting for the trap stiffness. To obtain measurements of DNA helix destabilization, the DNA was stretched in 100-nm steps and then held at a constant position while the resulting force as a function of time was measured. After capturing a single DNA molecule in the tethering buffer, the molecule was stretched to

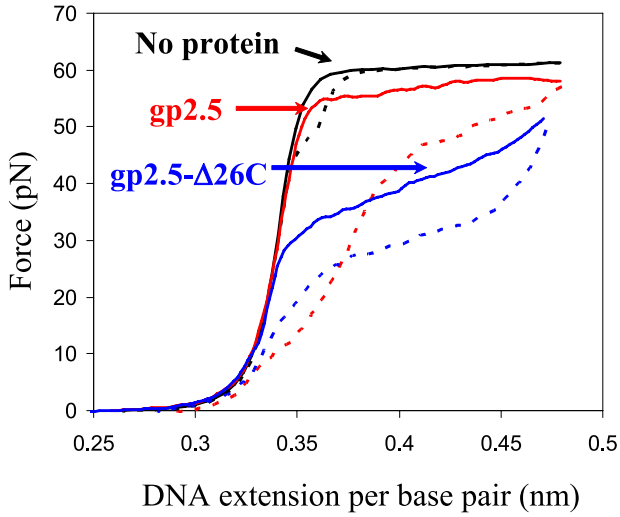

FIGURE 1. **λ-DNA stretching (*solid line*)-relaxation (*dashed line*) curves in 10 mM Hepes (pH 7. 5), 50 mM Na^+ (45 mM NaCl, 5 mM NaOH) in the absence of protein (*black*) and in the presence of 7 μM gp2.5 (*red*) and 300 nM gp2.5-Δ26C (*blue*).**

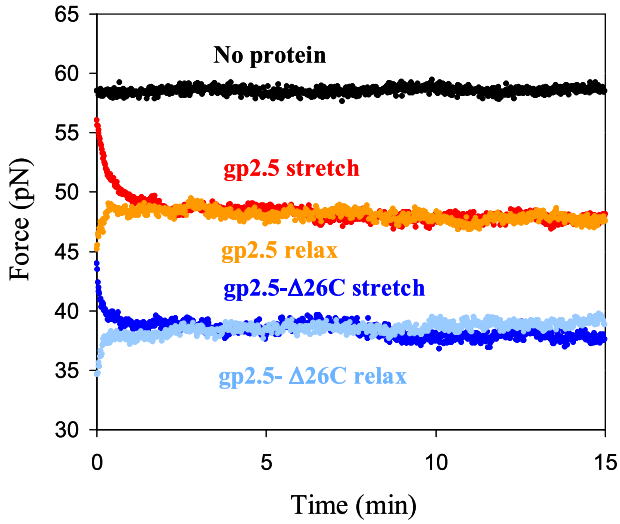

FIGURE 2. **Time dependence of the DNA stretching force at the midpoint of the melting transition in the absence of protein (*black*) and in the presence of 10 μM gp2.5 (*red*) and 80 nM gp2.5-Δ26C (*blue*) as well as the time dependence of DNA renaturation in which the DNA molecule has been overstretched and relaxed back to the same position in the presence of 10 μM gp2.5 (*light orange*) and 80 nM gp2.5-Δ26C (*light blue*).** Data were taken in 10 mM Hepes (pH 7.5), 25 mM Na^+ (20 mM NaCl, 5 mM NaOH).

verify that the usual force-extension curve was obtained and that only a single molecule had been tethered. To measure the effect of the protein on this transition, 4 to 5 cell volumes of a buffer solution containing a fixed amount of protein was added to the experimental cell until the buffer surrounding the captured DNA molecule had been completely exchanged.

RESULTS

Quantifying ssDNA Binding Affinity by Single Molecule Stretching—To probe the effect of these proteins on duplex DNA destabilization, we measured the force-extension curve of λ-DNA in the presence and absence of gp2.5 and gp2.5-Δ26C, a deletion mutant lacking 26 C-terminal amino acids, over a range of salt and protein concentrations. Typical results of our measurements in 50 mM Na^+ buffer are shown in Fig. 1. In the absence of protein, the DNA melting force is independent of pulling rate (12) and shows very little hysteresis. gp2.5 (7 μM) and gp2.5-Δ26C (300 nM) significantly lower the melting force relative to that observed in the absence of protein. However, much higher concentrations of gp2.5 compared with gp2.5-Δ26C are required to observe a significant reduction in the melting force. Although this behavior is expected for a protein that binds preferentially to ssDNA, this is the first observation of natural DNA denaturation in the presence of gp2.5. When the DNA was relaxed, the relaxation curves did not match the stretching curves, as shown by the *dashed lines* in Fig. 1. The considerable hysteresis shows that protein dissociation from exposed regions of ssDNA and subsequent DNA reannealing upon relaxation is slower than the 4-min duration of a stretching and relaxation cycle. In addition, lower rates of DNA stretching resulted in lower melting forces, signifying that the protein-ssDNA association and dissociation were slow on the time scale of the force-induced DNA melting.

Ideally, if we were able to pull slowly enough, we should be able to measure the complete equilibrium DNA stretching curve in the presence of the "slow" protein. However, our optical tweezers instrument does not allow pulling slower than 5–10 nm/s because of a position drift on longer time scales. Instead, we could measure the equilibrium force at the midpoint of the DNA melting transition. To this end, we rapidly stretched the dsDNA to a fixed end-to-end extension halfway between the dsDNA and ssDNA contour length and monitored the force, which converges to an equilibrium value, over a time scale of several minutes. This approach was used previously for equilibrium studies of T4 gene 32 protein interactions with DNA (11, 13). Typical results obtained in 25 mM Na^+ buffer are given in Fig. 2. After rapid stretching to the transition midpoint, the force decreased exponentially with time, representing additional DNA melting due to protein binding. The time-dependent force data can be fit to the following relation,

$$F(t)_{\text{stretch}} = F_m + (F_k - F_m)\exp\left(-\frac{t}{\tau_{\text{melt}}}\right) \qquad \text{(Eq. 1)}$$

where F_m is the equilibrium force obtained at long times, F_k is the initial melting force (the subscript k indicates that this kinetically determined force likely depends on pulling rate), and the constant τ_{melt} is the time for DNA melting due to protein binding. To measure the equilibrium force during the DNA renaturation, the DNA molecule was first stretched through the DNA melting transition and then relaxed quickly to the midpoint of the transition, and the change in force in the presence of each protein was monitored for at least 15 min. The observed force increased exponentially, representing DNA reannealing due to protein dissociation. The time-dependent force data upon relaxation were fit to an expression analogous to Equation 1. The fact that both denaturation and renaturation experiments converge to the same force, denoted by F_m, clearly demonstrates that the melting force obtained in the experiment outlined in Fig. 2 represents the equilibrium DNA melting force.

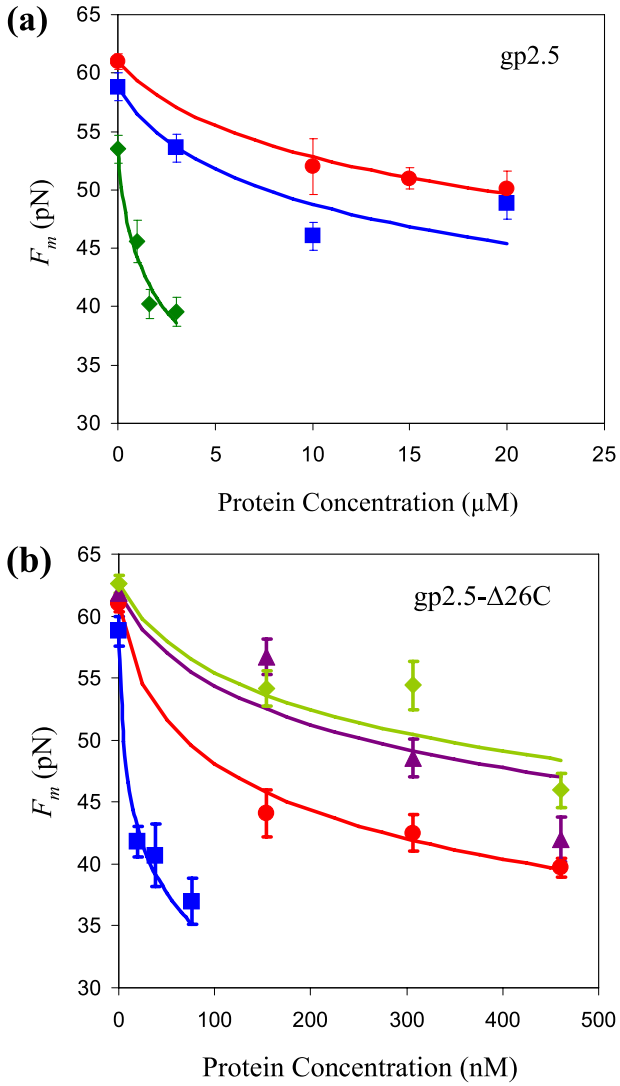

FIGUR 3. *a*, the measured DNA equilibrium melting force as a function of protein concentration, $F_m(C)$, for gp2.5. Measurements are shown in 0.005 M Na^+ (*filled green diamond*), 0.025 M Na^+ (*filled blue square*), and 0.05 M Na^+ (*filled red circle*). *b*, the measured DNA equilibrium melting force as a function of protein concentration, $F_m(C)$, for gp2.5-Δ26C. Measurements are shown in 0.025 M Na^+ (*filled blue square*), 0.05 M Na^+ (*filled red circle*), 0.075 M Na^+ (*filled violet triangle*), and 0.1 M Na^+ (*filled lime-green diamond*). *Lines* were fitted to data using Equation 4 and a χ^2 analysis. Each data point was obtained by averaging over three or more measurements, and the *error bars* were determined from the S.D. of those measurements.

As illustrated by Fig. 3, increasing amounts of either protein results in a lower DNA melting force, reflecting progressive protein-induced duplex destabilization. Below we use these data to determine the protein-DNA association constants of both proteins. The shift in the DNA melting temperature due to protein binding can be related to the protein-DNA binding constants to dsDNA and ssDNA as follows (41),

$$\frac{1}{T_m^0} - \frac{1}{T_m} = \frac{k_B}{\Delta H} \ln\left\{\frac{(1 + K_{ds}C)^{1/n_{ds}}}{(1 + K_{ss}C)^{1/n_{ss}}}\right\} \qquad \text{(Eq. 2)}$$

where n_{ss}, n_{ds}, K_{ss}, and K_{ds} are the binding site size in nucleotides and binding constants of the protein to ssDNA and dsDNA, respectively, and C is the bulk protein concentration. The change in DNA melting temperature and force due to duplex destabilization by protein can be related via general thermodynamics by the relation,

$$\Delta G_{\text{destabilization}} = (F_m - F_m^0)\Delta x = (T_m - T_m^0)\Delta S \qquad \text{(Eq. 3)}$$

where ΔS and Δx are the difference in entropy and extension per base pair between the protein-bound ssDNA and dsDNA, T_m^0, T_m, F_m^0, and F_m are the melting temperature and force in the absence and presence of protein, respectively, and $\Delta G_{\text{destabilization}}$ is the change in DNA melting free energy per base pair induced by protein binding. Combining Equations 2 and 3, using the relationship $\Delta H = \Delta S T_m^0$, and taking into the account that gp2.5 is a single-stranded binding protein, *i.e.* that $K_{ss} \gg K_{ds}$ (35), we can find the shift in melting force due to protein binding as follows.

$$F_m \approx F_m^0 - \frac{2k_BT}{n_{ss}\Delta x} \ln(1 + K_{ss}C) \qquad \text{(Eq. 4)}$$

By fitting the melting force as a function of concentration to Equation 4, we obtain a measurement of K_{ss} under the desired solution conditions. Below, we use this to examine the salt dependence of gp2.5 and gp2.5-Δ26C association to ssDNA.

Salt-dependent Binding of T7 gp2.5 and T7 gp2.5-Δ26C to ssDNA—Fitting the $F_m(C)$ data presented in Fig. 3 to Equation 4, we found K_{ss} for each protein at different salt concentrations. To perform this fit, we used our measured difference in length per base pair Δx between the dsDNA and ssDNA from the stretching curves for ssDNA in the presence of gp2.5-Δ26C in 0.005 M Na^+ buffer. This length change was not expected to depend significantly on ionic strength (8). Furthermore, by using the salt-independent parameter $n_{ss} = 7$ from the work of Kim *et al.* (35) and the salt-dependent value of DNA melting in the absence of the protein, F_m^0, from the work of Wenner *et al.* (5), we obtained the best fit to our data, which resulted in finding the binding constants for both proteins to ssDNA in different salt concentrations extended from 5 mM Na^+ to 50 mM Na^+ for gp2.5 and 25 mM Na^+ to 100 mM Na^+ for gp2.5-Δ26C.

As shown in Fig. 4, the C-terminal truncation of gp2.5 binds ssDNA about 100-fold stronger than the wild type gp2.5 in 100 mM Na^+ salt, in accord with previous data (35, 38). However, previous data were limited to a single measurement of $K_{ss} = 1.2 \times 10^6\ M^{-1}$ at 50 mM NaCl for gp2.5 by fluorescence quenching (35) compared with our measured value of $(3.5 \pm 0.6) \times 10^5\ M^{-1}$ at the same salt concentration. Similarly, previous data were limited to a single measurement of $K_{ss} = 3 \times 10^7\ M^{-1}$ at 50 mM KCl for gp2.5-Δ26C by electrophoretic mobility shift assay (38), which compares well with our measured value of $(7.8 \pm 0.9) \times 10^7\ M^{-1}$ in 50 mM Na^+ solution. For the electrophoretic mobility shift assay, we used the value obtained for binding to 70-base oligonucleotides as determined from the "slow mobility" lane of the gel. For this lane, the measured wild type gp2.5 value for K_{ss} agrees well with that measured in the earlier fluorescence quenching assay (35, 38).

Our measurements show that the ssDNA association constant of gp2.5-Δ26C depends much more strongly on salt than does that of wild type gp2.5, such that the stronger binding of the truncated protein becomes exaggerated in lower salt. Specifically, the total number of ions released upon protein binding, given by $n_{\text{Na}} = -d\log(K_{ss})/d\log(\text{Na}^+)$, is equal to $n_{\text{Na}} =$

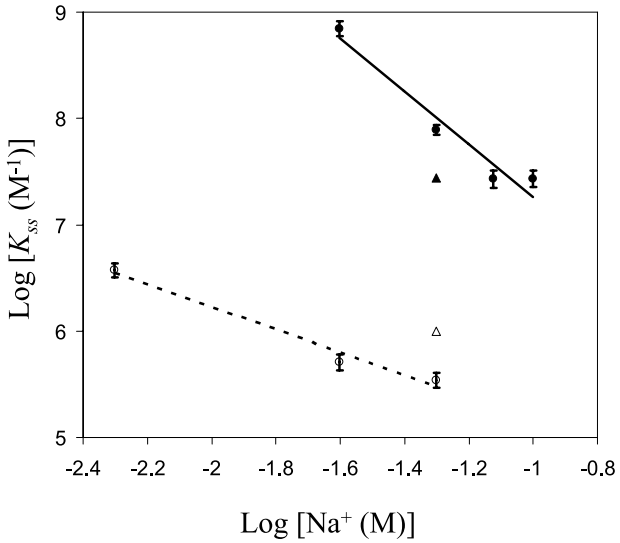

FIGURE 4. **The measured dependence of logarithm of the binding constant (K_{ss}) to ssDNA as a function of logarithm of salt concentration for gp2.5 (*open circle*) and gp2.5-Δ26C (*filled circle*) and the linear fit to the data for gp2.5 (*dashed line*) and gp2.5-Δ26C (*continuous line*).** The *open triangle* represents binding of gp2.5 to poly(dT) DNA at 50 mM NaCl using a fluorescence-based study by Kim *et al.* (35), and the *filled triangle* represents binding of gp2.5-Δ26C to 70-base oligonucleotides at 50 mM KCl using an electrophoretic mobility shift by Hyland *et al.* (38).

1.1 ± 0.1 for wild type and 2.5 ± 0.2 for the deletion mutant. Given that the deletion mutant, gp2.5-Δ26C, differs from the wild type protein, gp2.5, only by the absence of the last 26 C-terminal residues, it is surprising that the two binding constants differ so strongly. Below, under "Discussion," we present a model for regulation of gp2.5-DNA binding by a dimerization interaction involving the C terminus, which could potentially explain this unusual result.

DISCUSSION

Using single molecule DNA FIM in the presence of gp2.5 and gp2.5-Δ26C, we have determined the binding affinity of both proteins as a function of salt concentration. We find that in low salt, the binding affinity of gp2.5-Δ26C for ssDNA exceeds that of gp2.5 by 2–3 orders of magnitude. In addition, the binding affinities for both proteins are salt-dependent, and the salt dependence of gp2.5-Δ26C binding to DNA is much stronger. Because gp2.5-Δ26C lacks only the C terminus of gp2.5, this result shows that the presence of the C terminus on gp2.5 reduces its affinity for DNA. The C terminus of gp2.5 is flexible and may extend away from the β-barrel of the OB-fold into solution. However, acidic and aromatic residues of the C-terminal tail make it an ideal mimic of ssDNA. Therefore, one possible mechanism for this reduction in binding affinity is the electrostatic binding of the C terminus to the DNA binding site. If this were the case, the C terminus would compete with ssDNA for binding to the cationic DNA binding site, which would result in weaker binding to DNA in lower salt relative to a protein lacking the C terminus. Such a salt-dependent DNA binding regulation mechanism was recently reported for bacteriophage T4 gene 32 protein, the ssDNA-binding protein for T4 (13, 18). However, gp2.5 is known to form a dimer in solution, whereas gp2.5-Δ26C has not been observed to form dimers in solution; thus any model for gp2.5 binding must take this dimerization interaction into account.

Based on the lack of dimerization for gp2.5-Δ26C in solution, it has been suggested previously that the C-terminal segments stabilize the dimer form of gp2.5 by a domain swapping interaction (42) across the dimer interface (39, 40), as illustrated in Fig. 5*b*. This model resembles the model described above for electrostatic regulation of DNA binding by the C terminus, but in this case DNA binding requires dimer dissociation by which the C terminus is removed from the DNA binding site of each protein. This interaction is more complex than that suggested for T4 gene 32 protein, because the dimer formation likely involves more interactions than just the C termini binding to the DNA binding sites. In particular, there is an additional dimer interface that contributes to the overall dimerization interaction and that also must be disrupted for DNA binding by gp2.5 to occur (40). In the case of T4 gp32, a C-terminal truncation, *I, showed a strong salt dependence at low salt, yielding a value of $n_{Na} = 3$, similar to that observed here for gp2.5-Δ26C. In contrast, wild type T4 gp32 showed very little salt dependence, with $n_{Na} \simeq 0$. This is similar to that observed for wild type gp2.5. However, in the case of T4 gp32, the association constants for both *I and wild type gp32 converged at 200 mM NaCl. This suggests that above 200 mM NaCl, the C-terminal domain of gp32 spends most of its time in solution. In turn, this result reveals that the binding of the gp32 C-terminal domain to its DNA binding site, which regulates its DNA binding, is an entirely electrostatic effect that is screened at salt concentrations above 200 mM. In contrast, the results on gp2.5 and gp2.5-Δ26C reported here show that the inhibition of binding by the gp2.5 C-terminal tail persists even at 1 M NaCl. Therefore, the interactions that are responsible for the difference in gp2.5 and gp2.5-Δ26C binding must have a nonelectrostatic component, in contrast to the interactions that determine the difference between T4 gp32 and *I binding. The additional requirement for breaking the gp2.5 dimer interface, discussed below, is sufficient to explain this difference between the salt dependence of T4 gp32-DNA binding relative to the DNA binding of T7 gp2.5.

Although our data alone cannot prove the above model of gp2.5 dimerization and ssDNA binding, our results are fully consistent with the model and provide further support for it. There are two likely scenarios for gp2.5 binding. One possibility is that the C terminus of one monomer is removed from the DNA binding site and exposed to solution, whereas the other monomer binds DNA. A second possibility is that the dimer dissociates, with both C-terminal tails removed from the DNA binding pocket of the other protein. Below, we used our data on gp2.5 and gp2.5-Δ26C binding to ssDNA over a broad range of salt concentrations to quantitatively probe the salt-dependent gp2.5 interaction that regulates gp2.5 binding to DNA. We show that this interaction consists of two components: electrostatic, representing the release of the C-terminal tail, and nonelectrostatic, which likely represents dissociation at the dimer interface. A schematic diagram of the model describing these interactions is shown in Fig. 5. The fact that we see a significant nonelectrostatic component to the interaction energy that regulates gp2.5 binding supports a model in which a breaking of the dimer interface is required for gp2.5 binding. However,

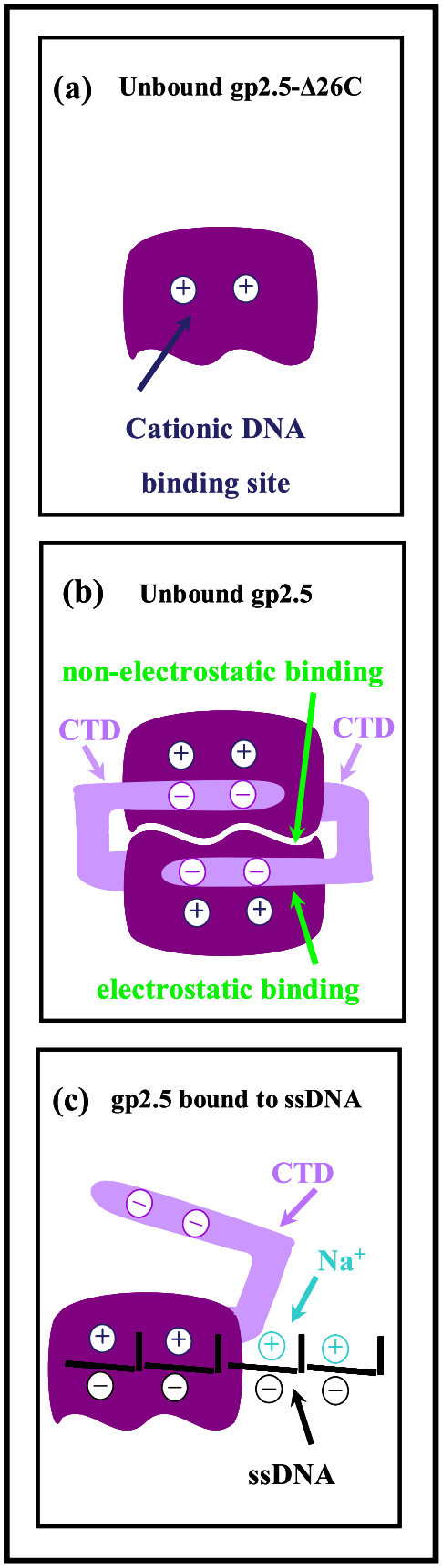

FIGURE 5. **Schematic diagram of the model for gp2.5 dimer formation, which must be broken prior to DNA binding.** *a*, for gp2.5-Δ26C, the DNA binding site is always available for DNA binding because of the lack of the C-terminal tail. *b*, C-terminal tails stabilize the gp2.5 dimer by their "domain swap," *i.e.* binding to the basic regions of its gp2.5 partner. The gp2.5 cationic binding site for its partner's C-terminal tail is also its ssDNA binding site. Therefore, gp2.5 is monomeric in its DNA-bound state and dimeric in its unbound state. *c*, a conformational change in gp2.5 involving dimer dissociation is required prior to gp2.5 nucleic acid binding. *CTD*, C-terminal domain.

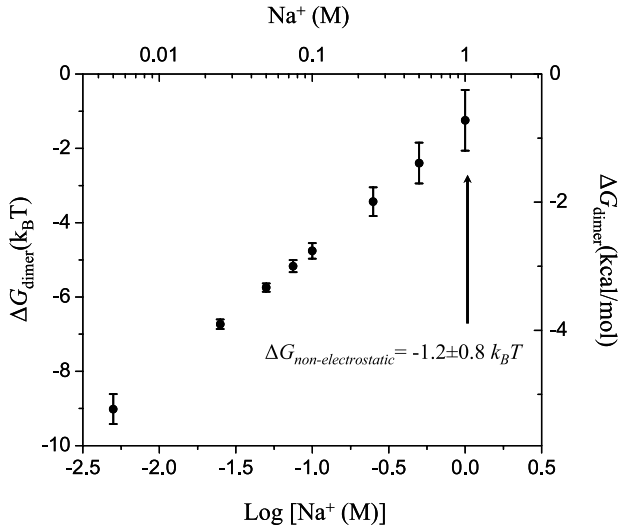

FIGURE 6. **The free energy of dimerization measured as a function of the logarithm of salt concentration.** Using the binding constants of gp2.5 and gp2.5-Δ26C to ssDNA in 25 and 50 mM Na^+ buffer, we determined the values of ΔG_{dimer} directly. By extrapolating the salt-dependent data for each protein separately, we were able to calculate ΔG_{dimer} in other salt concentrations. The *arrow* shows the value of the non-electrostatic component of ΔG_{dimer}.

without additional evidence we cannot completely exclude nonelectrostatic interactions between the C-terminal tail and the DNA binding site, which might allow for very weak gp2.5 dimerization when bound to DNA.

If the DNA binding of gp2.5 differs from gp2.5-Δ26C binding only because of a requirement of dimer dissociation, and the dimer interaction is in pre-equilibrium to DNA binding, then the binding affinity of gp2.5 compared with that of gp2.5-Δ26C is reduced by the probability of dimer dissociation, P_{dimer},

$$K_{ss}^{gp2.5} = K_{ss}^{gp2.5\text{-}\Delta26C} \times P_{dimer} \qquad \text{(Eq. 5)}$$

where $K_{ss}^{gp2.5}$ and $K_{ss}^{gp2.5\text{-}\Delta26C}$ are the association constants of gp2.5 and gp2.5-Δ26C to ssDNA, respectively, and equation as follows.

$$P_{dimer} = \frac{e^{\Delta G_{dimer}/k_BT}}{e^{\Delta G_{dimer}/k_BT} + 1} \qquad \text{(Eq. 6)}$$

Here ΔG_{dimer} is the attractive (negative) free energy of gp2.5 dimerization per dimer, which can be obtained by solving Equations 5 and 6.

$$\Delta G_{dimer} = -k_BT \ln (K_{ss}^{gp2.5\text{-}\Delta26C}/K_{ss}^{gp2.5} - 1) \qquad \text{(Eq. 7)}$$

The gp2.5 dimerization free energy as a function of salt in the range of 5 to 100 mM Na^+, obtained according to Equation 7 using our measured binding constants for both proteins, is presented in Fig. 6. We find that ΔG_{dimer} is strongly salt-dependent, in agreement with the significant contribution to gp2.5 dimerization from the electrostatically driven C-terminal tail

(CTT) swap between gp2.5 monomers. Indeed, the electrostatic similarity between the CTT and the region of ssDNA that binds gp2.5 implies that gp2.5 dimerization should be almost as salt dependent as binding of gp2.5-Δ26C to ssDNA. An analogous salt-dependent CTT unbinding from the ssDNA binding groove of T4 gene 32 protein was described recently (13, 18). Quantitatively, this means that one might expect $d\Delta G_{\mathrm{dimer}}/d\ln(\mathrm{Na}^+)$ to be similar in magnitude and opposite in sign to $d\ln(K_{ss}^{\mathrm{gp2.5\text{-}\Delta 26C}})/d\ln(\mathrm{Na}^+)$. Experimentally, we find that $d\Delta G_{\mathrm{dimer}}/d\ln(\mathrm{Na}^+) \approx 1.4 \pm 0.1$ and $-d\ln(K_{ss}^{\mathrm{gp2.5\text{-}\Delta 26C}})/d\ln(\mathrm{Na}^+) \approx 2.5 \pm 0.1$. This result suggests that the CTT is highly charged but somewhat less charged than the section of ssDNA that binds gp2.5.

In ~1 M salt, all electrostatic interactions are significantly screened by salt ions, and the remaining interactions reflect their non-electrostatic salt-independent component (43). Therefore, extrapolating $\Delta G_{\mathrm{dimer}}(\mathrm{Na}^+)$ to 1 M Na^+, we obtained an estimate of the non-electrostatic component of the gp2.5 dimerization free energy $\Delta G_{\mathrm{dimer}} = (-1.2 \pm 0.8)\ k_BT = 0.7 \pm 0.4$ kcal/mol. This weak dimer interaction explains why gp2.5-Δ26C does not form dimers in solution but crystallizes as a dimer (39). The CTT swap makes gp2.5 dimerization progressively stronger in lower salt. However, even at the physiological salt concentration of ~100 mM, the dimerization free energy is moderate, at approximately $-5\ k_BT$ and −3 kcal/mol, and should not completely preclude thermal dimer dissociation, which is required for gp2.5 binding to ssDNA.

In a previous study, Rezende *et al.* (40) examined gp2.5, gp2.5-Δ26C, and several mutants at the dimerization interface by gel filtration in 50 mM KPO_4 (pH 7.0), 0.1 mM EDTA, 0.1 mM dithiothreitol, and 10% glycerol buffer at a single protein concentration. Several salt concentrations were examined: 150, 250, and 500 mM NaCl. gp2.5C-Δ26C was reported to be a monomer at all salt concentrations, and gp2.5 was reported to be a dimer at 150 and 250 mM and a monomer at 500 mM NaCl. The mutants at the dimerization interface were reported to be dimers at 150 mM NaCl and monomers at 250 and 500 mM NaCl. These results are consistent with our model of gp2.5 dimerization in which most of the dimerization free energy comes from the electrostatic interactions of the anionic C-terminal tails of the protein with the cationic ssDNA binding site on the dimerization partner. Although dimerization becomes weaker with increasing salt concentration, it also requires interactions at the dimer interface. The fact that the gel filtration study suggests that dimer dissociation occurs at 0.5 M NaCl, in contrast to our prediction of a marginally stable dimer at 1 M NaCl, is likely because of the lower protein concentration used in the gel filtration study.

According to previous studies (22–26) the CTT of gp2.5 is known to interact with several components of the T7 replication fork. Therefore, it is possible that these interactions regulate CTT-induced gp2.5 dimerization, thereby controlling gp2.5 binding to ssDNA at the replication fork. Such control may have an important regulatory role, by preventing the extensive gp2.5 binding and accompanying melting of double-stranded DNA that is not involved in replication. Alternatively, exposure of the C terminus upon gp2.5 binding to DNA could itself regulate the activities of other proteins at the replication fork. Further studies of gp2.5 interactions with DNA and other replication proteins are needed to distinguish between these possibilities and elucidate the critical interactions between components of the model T7 DNA replication machinery.

In summary, we have quantitatively determined the affinity of gp2.5 and gp2.5-Δ26C binding to DNA as a function of salt concentration. We find that gp2.5 binding is regulated by electrostatic interactions involving the C terminus, in addition to a weak non-electrostatic binding component. We have presented a model in which protein dimerization involving the C terminus regulates DNA binding by gp2.5. Our model suggests that, although the dimerization interaction is primarily electrostatic, there is a weak non-electrostatic component, which likely represents interactions at the dimer interface.

Acknowledgment—We thank Micah McCauley for instrumentation assistance and preparation of labeled DNA.

REFERENCES

1. Bustamante, C., Smith, S. B., Liphardt, J., and Smith, D. (2000) *Curr. Opin. Struct. Biol.* **10,** 279–285
2. Bustamante, C., Bryant, Z., and Smith, S. B. (2003) *Nature* **421,** 423–427
3. Strick, T., Allemand, J., Croquette, V., and Bensimon, D. (2000) *Prog. Biophys. Mol. Biol.* **74,** 115–140
4. Allemand, J. F., Bensimon, D., and Croquette, V. (2003) *Curr. Opin. Struct. Biol.* **13,** 266–274
5. Wenner, J. R., Williams, M. C., Rouzina, I., and Bloomfield, V. A. (2002) *Biophys. J.* **82,** 3160–3169
6. Williams, M. C., and Rouzina, I. (2002) *Curr. Opin. Struct. Biol.* **12,** 330–336
7. Rouzina, I., and Bloomfield, V. A. (2001) *Biophys. J.* **80,** 882–893
8. Rouzina, I., and Bloomfield, V. A. (2001) *Biophys. J.* **80,** 894–900
9. Williams, M. C., Rouzina, I., and Bloomfield, V. A. (2002) *Acc. Chem. Res.* **35,** 159–166
10. Williams, M. C., Wenner, J. R., Rouzina, I., and Bloomfield, V. A. (2001) *Biophys. J.* **80,** 874–881
11. Pant, K., Karpel, R. L., and Williams, M. C. (2003) *J. Mol. Biol.* **327,** 571–578
12. Pant, K., Karpel, R. L., Rouzina, I., and Williams, M. C. (2004) *J. Mol. Biol.* **336,** 851–870
13. Pant, K., Karpel, R. L., Rouzina, I., and Williams, M. C. (2005) *J. Mol. Biol.* **349,** 317–330
14. Krautbauer, R., Fischerländer, S., Allen, S., and Gaub, H. E. (2002) *Single Mol.* **3,** 97–103
15. Krautbauer, R., Pope, L. H., Schrader, T. E., Allen, S., and Gaub, H. E. (2002) *FEBS Lett.* **510,** 154–158
16. Mihailovic, A., Vladescu, I., McCauley, M., Ly, E., Williams, M. C., Spain, E. M., and Nunez, M. E. (2006) *Langmuir* **22,** 4699–4709
17. Vladescu, I. D., McCauley, M. J., Rouzina, I., and Williams, M. C. (2005) *Phys. Rev. Lett.* **95,** 158102
18. Rouzina, I., Pant, K., Karpel, R. L., and Williams, M. C. (2005) *Biophys. J.* **89,** 1941–1956
19. Williams, M. C., Rouzina, I., and Karpel, R. L. (2006) *Curr. Org. Chem.* **10,** 419–432
20. Lohman, T. M., and Ferrari, M. E. (1994) *Annu. Rev. Biochem.* **63,** 527–570
21. Chase, J. W., and Williams, K. R. (1986) *Annu. Rev. Biochem.* **55,** 103–136
22. Kim, Y. T., Tabor, S., Churchich, J. E., and Richardson, C. C. (1992) *J. Biol. Chem.* **267,** 15032–15040
23. Kong, D., and Richardson, C. C. (1998) *J. Biol. Chem.* **273,** 6556–6564
24. Kim, Y. T., and Richardson, C. C. (1994) *J. Biol. Chem.* **269,** 5270–5278
25. He, Z.-G., Rezende, L. F., Willcox, S., Griffith, J. D., and Richardson, C. C. (2003) *J. Biol. Chem.* **278,** 29538–29545
26. He, Z.-G., and Richardson, C. C. (2004) *J. Biol. Chem.* **279,** 22190–22197
27. Araki, H., and Ogawa, H. (1981) *Mol. Gen. Genet.* **183,** 66–73

28. Scherzinger, E., Litfin, F., and Jost, E. (1973) *Mol. Gen. Genet.* **123,** 247–262
29. Kim, Y. T., and Richardson, C. C. (1993) *Proc. Natl. Acad. Sci. U. S. A.* **90,** 10173–10177
30. Reuben, R. C., and Gefter, M. L. (1973) *Proc. Natl. Acad. Sci. U. S. A.* **70,** 1846–1850
31. Kong, D., and Richardson, C. C. (1996) *EMBO J.* **15,** 2010–2019
32. Kong, D., Nossal, N. G., and Richardson, C. C. (1997) *J. Biol. Chem.* **272,** 8380–8387
33. Kong, D., Griffith, J. D., and Richardson, C. C. (1997) *Proc. Natl. Acad. Sci. U. S. A.* **94,** 2987–2992
34. Nakai, H., and Richardson, C. C. (1988) *J. Biol. Chem.* **263,** 9831–9839
35. Kim, Y. T., Tabor, S., Bortner, C., Griffith, J. D., and Richardson, C. C. (1992) *J. Biol. Chem.* **267,** 15022–15031
36. Yu, M., and Masker, W. (2001) *J. Bacteriol.* **183,** 1862–1869
37. Rezende, L. F., Willcox, S., Griffith, J. D., and Richardson, C. C. (2003) *J. Biol. Chem.* **278,** 29098–29105
38. Hyland, E. M., Rezende, L. F., and Richardson, C. C. (2003) *J. Biol. Chem.* **278,** 7247–7256
39. Hollis, T., Stattel, J. M., Walther, D. S., Richardson, C. C., and Ellenberger, T. (2001) *Proc. Natl. Acad. Sci. U. S. A.* **98,** 9557–9562
40. Rezende, L. F., Hollis, T., Ellenberger, T., and Richardson, C. C. (2002) *J. Biol. Chem.* **277,** 50643–50653
41. McGhee, J. D. (1976) *Biopolymers* **15,** 1345–1375
42. Bennett, M. J., Schlunegger, M. P., and Eisenberg, D. (1995) *Protein Sci.* **4,** 2455–2468
43. Record, M. T., Jr., Anderson, C. F., and Lohman, T. M. (1978) *Q. Rev. Biophys.* **11,** 103–178